Title

Metabolism of ticlopidine in rats: Identification of the main biliary metabolite as a GSH conjugate of ticlopidine S-oxide

Shinji Shimizu, Ryo Atsumi, Tsunenori Nakazawa, Yuko Fujimaki, Kenichi Sudo, and Osamu Okazaki

Drug Metabolism and Pharmacokinetics Research Laboratories, Daiichi Sankyo Co., Ltd. 1-2-58, Hiromachi, Shinagawa-ku, Tokyo 140-8710, Japan.

DMD Fast Forward. Published on June 18, 2009 as DOI: 10.1124/dmd.109.027524
This article has not been copyedited and formatted. The final version may differ from this version.

Running title

a) Running title: Metabolism of ticlopidine

b) Correspondence: Shinji Shimizu

Address: 1-2-58, Hiromachi, Shinagawa-ku, Tokyo 140-8710, Japan.

Telephone: +81-3-3492-3131

Facsimile: +81-3-5436-8567

E-mail address: shimizu.shinji.d3@daiichisankyo.co.jp

c) The number of text page: 21

The number of tables: 0

The number of figures: 13

The number of references: 26

The number of words in Abstract: 142

The number of words in Introduction: 232

The number of words in Discussion: 1217

d) A list of nonstandard abbreviations: 0

DMD Fast Forward. Published on June 18, 2009 as DOI: 10.1124/dmd.109.027524
This article has not been copyedited and formatted. The final version may differ from this version.

ABSTRACT

We have identified several novel metabolites of ticlopidine, a well-known anti-platelet agent, and have revealed its metabolic route in rats. The main biliary metabolite of ticlopidine was characterized as a GSH conjugate of ticlopidine S-oxide, in which conjugation had occurred at carbon 7a in the thienopyridine moiety. Quantitative analysis revealed that 29% of the dose was subjected to the formation of reactive intermediates followed by conjugation with GSH after oral administration of ticlopidine (22 mg /kg) to rats. In vitro incubation of ticlopidine with rat liver S9 fractions led to the formation of multiple metabolites, including 2-oxo-ticlopidine, the precursor for the pharmacologically active ticlopidine metabolite, [1-(2-chlorobenzyl)-4-mercaptopiperidin-(3Z)-ylidene]-acetic acid. A novel thiophene-ring opened metabolite with a thioketone group and a carboxylic acid moiety has also been detected after incubation of 2-oxo-ticlopidine with rat liver microsomes or upon incubation of ticlopidine with rat liver S9 fractions.

DMD Fast Forward. Published on June 18, 2009 as DOI: 10.1124/dmd.109.027524
This article has not been copyedited and formatted. The final version may differ from this version.

Introduction

Ticlopidine is a well-known anti-platelet agent (Quinn and Fitzgerald, 1999) and has been widely used for the secondary prevention of atherothrombosis (Jacobson, 2004). The metabolism of ticlopidine is complex due to extensive oxidation in the liver (Saltile and Ward, 1987). For example, less than 1% of the parent compound was detected in urine, whereas about 60% and 25% of radioactivity was recovered in urine after a single oral administration of [^{14}C]-ticlopidine to humans (Noble and Goa, 1996) and rats (Tuong et al, 1981), respectively. Furthermore, a large difference was observed between the total radioactivity and unchanged ticlopidine in the plasma level (Panak et al., 1983). In 1980s, the metabolic studies suggested that N-dealkylation, N-oxidation, and oxidation of the thiophene ring followed by ring opening appeared to be the main routes, but numerous highly polar urinary and biliary metabolites in both humans and animals remained unidentified (Tuong et al, 1981; Panak et al., 1983). Recently, novel ticlopidine metabolites such as the S-oxide form (Ha-Duong et al., 2001) and the pharmacologically active metabolite (Yoneda et al., 2004) have been detected. However, the whole metabolism of ticlopidine has remained unclarified.

In the present study, we have identified several novel metabolites of ticlopidine and revealed the metabolic pathways of ticlopidine quantitatively. Moreover, an in vitro experiment was conducted in order to elucidate the whole metabolic route of ticlopidine including the biotransformation to the pharmacologically active metabolite.

Materials and Methods

Chemicals. Ticlopidine: 5-(2-Chloro-benzyl)-4,5,6,7-tetrahydro-thieno[3,2-c]pyridine, Ticlopidine N-oxide: 5-(2-Chloro-benzyl)-6,7-dihydro-4H-thieno[3,2-c]pyridine 5-oxide, Ticlopidine pharmacologically active metabolite: [1-(2-Chloro-benzyl)-4-mercapto-piperidin-(3Z)-ylidene]-acetic acid, THTP: 4,5,6,7-tetrahydrothieno-[3,2-c]pyridine, and 2-oxo ticlopidine: 5-(2-Chloro-benzyl)-

5,6,7,7a-tetrahydro-4H-thieno[3,2-c]pyridin-2-one were chemically synthesized. [^{14}C]-ticlopidine (>99% by HPLC and 97.3% by TLC) was synthesized at Daiichi Pure Chemicals Co., Ltd. (Ibaraki, Japan, Fig. 1). Glucose-6-phosphate (G6P) and glutathione (GSH) were obtained from Sigma Co., Ltd. (Tokyo, Japan), glucose-6-phosphate dehydrogenase (G6PDH) and β-nicotinamide-adenine dinucleotide phosphate, oxidized form, and monosodium salt ($NADP^+$) were obtained from Oriental Yeast Co., Ltd. (Tokyo, Japan).

$MgCl_2$•$6H_2O$ and β-naphthoflavone were obtained from Nacalai Tesque, Inc. (Kyoto, Japan). Phenobarbital sodium salt was obtained from Wako Pure Chemical Industries Co., Ltd. (Osaka, Japan). Acetonitrile (Kanto Chemical Co., Inc., Tokyo, Japan) was HPLC grade, and all other chemical reagents were of the highest grade commercially available.

Animals. 6-week-old SD male rats were purchased from Japan SLC, Inc. (Shizuoka, Japan). The rats were housed at a constant temperature (23 ± 2°C) and humidity (55 ± 20%) under a 12 h light/dark cycle. The rats were given food (Funahashi F-2, Funahashi Farm, Chiba, Japan) and water ad libitum.

Administration and sample collection. Animal surgery for the collection of bile and urine was conducted based on that previously reported (Ito et al., 2007) with slight modification. Briefly, each rat was anesthetized with diethyl ether in a fasting condition and had a polyethylene cannula (PE-10, Becton Dickinson Co.,. Franklin Lakes, NJ) surgically inserted into the common bile duct, was fitted a penis tube to collect urine, and then was individually housed in a restraining cage (Bollman cage, SUGIYAMA-GEN IRIKI Co.,Ltd., Tokyo, Japan). After recovery from the anesthesia (about 30 min after completion of the surgery), the animals were orally treated with [^{14}C]-ticlopidine (22 mg/9.88 MBq/kg) in distilled water (2.5 mL/kg) by gavage tube. Bile and urine were collected during the periods of 0-15 h and 15-20 h after administration. 5.15 to 12.9 mL of bile was collected during 0-20 h for each rat. (The bile flow rate was 0.258 to 0.645 mL/h.)

Measurement of radioactivity. A 20-μL aliquot of each bile and urine sample was placed into separate liquid scintillation vials. Then, 10 mL of a liquid scintillation solution (AQUASOL-2, Packard

BioScience, Wellesley, MA) was added before measurement of the radioactivity using a liquid scintillation counter (LSC-3500, Aloka, Tokyo, Japan).

Radio-HPLC analysis. After filtering through an ULTRAFREE®-MC 0.22 μm Filter Unit (Millipore, Billerica, MA), aliquot of 30 to 40-μL bile or urine samples were loaded onto an HPLC column Symmetry C_{18}, 5 μm, 150 mm x 4.6 mm I.D. (Waters, Milford, MA). The column temperature was 40°C. The mobile phase consisted of a linear gradient of solvent A (10 mM CH_3COONH_4) and solvent B (CH_3CN) according to the following program: B (%), 10 (0-5 min) - 75 (23-29 min) - 10 (30 min). The HPLC system consisted of an L-4000 UV Detector (Hitachi, Tokyo, Japan) and L-6200 Intelligent Pump (Hitachi) set at a flow rate of 1 mL/min. A radio-HPLC system, β-RAM model 3 radioactivity detector (IN/US System, Tampa, FL), was used for the radioactive detection. Metabolites were quantified by integration of the peaks found in the radiochromatogram during the radio-HPLC analysis, assuming that all the radioactivity in bile and urine could be analyzed on the radiochromatogram, since the extraction efficiencies of radioactivity from the bile and urine sample were determined to be more than 99% in our preliminary experiment, where one bile sample and one urine sample were drawn as representative to ascertain the extraction efficiency of radioactivity.

Preparation of rat liver S9 and microsomes. Rat liver S9 and microsomes were prepared from 7-week-old male Wistar rats (Japan SLC, Inc.) treated with β-naphthoflavone (80 mg/kg, 2 mL/kg, once daily, suspended in corn oil) for 2 days followed by treatment with phenobarbital (60 mg/kg, 2 mL/kg, once daily, in 0.9 % [w/v] sodium chloride) for 3 days. The rats were sacrificed by cervical dislocation and the liver of each rat was immediately removed. The livers were perfused with an ice-cold 1.15% [w/v] potassium chloride solution and were then minced and pooled. The pooled liver tissues (139 g in total) were homogenized in 240 mL of the ice-cold 1.15% potassium chloride solution. The homogenates were centrifuged (AvantiTM HP-25, Beckman, Fullerton, CA) at 9,000 *g* for 20 min at 4°C and a part of the supernatant was then stored as liver S9 at -80°C. The remaining supernatant fractions were further centrifuged (SCP70H2, Hitachi) at 105,000 *g* for 1 h at 4°C. The resulting microsomal pellets were washed with 0.1 M sodium phosphate buffer (pH 7.4) and recentrifuged at

105,000 *g* for 1 h at 4°C. The pellets were then resuspended in a small volume of 0.1 M sodium phosphate buffer (pH 7.4) and stored at -80°C. A standard Lowry assay kit (DC Protein Assay Kit 2, Bio-Rad, Hercules, CA) was used to measure the rat liver S9 and microsomal protein concentrations.

In vitro metabolic study. The reaction mixtures contained the following components: 100 mM sodium phosphate buffer (pH 7.4), rat liver 9,000 *g* supernatant fraction (S9) or rat liver microsomal fraction (2 mg protein/mL), ticlopidine or 2-oxo ticlopidine (1 mM), G6P (10 mM), G6PDH (1 units/mL), $MgCl_2$ (4 mM), GSH (5 mM), and $NADP^+$ (1 mM). Each reaction was started by the addition of S9 or microsomes after a 2-min pre-incubation at 37°C. After 60 or 120 minutes of incubation, the reaction was terminated by adding a 2 fold volume of ice-cold CH_3CN. The samples were mixed with a vortex mixer and centrifuged (MX-300, TOMY, Tokyo, Japan) at 9,100 *g* for 20 min at 4°C. Each supernatant was recentrifuged at 9,100 *g* for 5 min at 4°C. Each resulting supernatant was collected separately and analyzed by LC/MS and LC/MS/MS.

LC/MS and LC/MS/MS analysis. The in vitro reaction mixtures were analyzed by LC/MS and LC/MS/MS on an Alliance 2690 HPLC system (Waters) coupled to a Finnigan LCQ ion trap mass spectrometer (ThermoQuest, San Jose, CA) in positive ion electrospray mode. The analytical conditions (column and mobile phase) were the same as those described above in the radio-HPLC system. The capillary heater was set to 250°C. For the MS/MS experiments the relative collision energy was set at 20-40%.

Preparation of the sample for isolation of the main biliary metabolite. Isolation was conducted using the bile sample from 10 rats administered non-radiolabeled ticlopidine (26 mg/kg) in distilled water (2.5 mL/kg). Bile samples were collected for 16 h after administration. Each biliary sample was pooled and applied (10 mL x 7) to solid phase extraction columns (Mega Bond Elut C_{18} 60CC/10GRM, Varian, Palo Alto, CA). After washing with 5% CH_3CN /10 mM CH_3COONH_4 (75 mL), the metabolites were eluted with 20% CH_3CN /10 mM CH_3COONH_4 (75 mL). This solution was freeze-dried and the residue was dissolved in distillated water (20 mL) and subjected to the preparative HPLC.

Preparation of the sample for isolation of in vitro metabolites. For isolation of in vitro ticlopidine metabolites, a large-scale incubation using rat liver microsomes was conducted. The reaction mixture contained 50 mM Tris-HCl buffer (pH 7.5), rat microsomal protein (1 mg protein/mL), ticlopidine (666 μM), G6P (10 mM), G6PDH (1 units/mL), $MgCl_2$ (4 mM), and $NADP^+$ (1 mM). The total volume of the reaction mixture was 500 mL (1 mL x 500 tubes). The reactions were started by the addition of $NADP^+$ after a 3-min pre-incubation at 37°C. After 30 minutes of incubation, the reactions were terminated by treatment with an equal volume of ice-cold $CH_3COOCH_2CH_3$. Each mixture was pooled and vigorously shaken to extract the metabolites. After evaporation of the organic solvent under reduced pressure, the resulting residue was dissolved in CH_3CN. The fractions containing metabolites were subjected to the preparative HPLC described below.

Preparative HPLC. Isolation of metabolites was performed with a Hitachi D-7000 HPLC system, which consists of a L-4000 UV Detector and L-7100 Pump (Hitachi) set at a flow rate of 2.8 mL/min. Symmetry C_{18} column (7 μm, 300 mm x 7.8 mm I.D., Waters) was used for the separation. The mobile phase consisted of solvent A (10 mM CH_3COONH_4) and solvent B (CH_3CN). To separate the biliary metabolite, the following linear gradient programs were used: B, 15% (0-2 min) – 50% (18-20 min) – 15% (23 min) for rough separation and then 15% (0-20 min) – 50% (25-27 min) – 15% (29 min) for complete separation. To isolate the in vitro metabolites, the following linear gradient program: B, 40% (0 min) – 75% (10-25 min) – 40% (28 min) was used for rough fractionation. The resulting fraction containing in vitro metabolites was subjected to isocratic elution (B, 45%) for complete separation.

Characterization of isolated metabolites. ^{1}H-NMR, ^{1}H-^{1}H COSY NMR, ^{13}C-NMR, and ^{1}H-^{13}C COSY NMR analysis were performed using a JNM-ECP500 NMR spectrometer (JEOL, Tokyo, Japan). Deuterated water (D_2O) was used as a solvent for the biliary metabolite, and chemical shifts (δ) were expressed as parts per million downfield from the internal standard of sodium 3-trimethylsilylpropionate-2, 2, 3, 3, -d4 (TSP). For the in vitro metabolites, deuterium methanol (CD_3OD) was used as a solvent. Chemical shifts (δ) are expressed as parts per million downfield from the internal standard of tetramethylsilane (TMS). MS and MS/MS analyses were conducted using a

Finnigan LCQ ion trap mass spectrometer. MS conditions were the same as those described in the LC/MS and LC/MS/MS analyses.

Results

Biliary and urinary excretion of [^{14}C]-ticlopidine. The cumulative biliary excretion of radioactivity during the 0-15 h collection period was 46.6 ± 10.1% of the dose given (n=9), and slightly increased to 48.1 ± 10.1% up to 20 h (n=9). The cumulative urinary excretion of radioactivity during the 0-15 h collection period was 12.9 ± 0.3% of the dose given (n=3) and slightly increased to 14.1% up to 20 h (n=2). (Only 2 or 3 rats could be used for the measurement of urinary excretion because the penis tubes to collect urine were detached in 6 out of 9 animals during 0-15 h after administration, and one more rat lost its tube during 15-20 h after administration.)

Radio-HPLC profiles of biliary and urinary metabolites. Fig. 2A shows representative radio chromatogram of bile collected 0-15 h after [^{14}C]-ticlopidine administration. Two main peaks, metabolite B1 and metabolite B2, were detected at retention times (RT) of 12.0 min and 13.2 min, respectively. The metabolite (RT: 16.4 min) was identified as ticlopidine N-oxide by comparison with an authentic standard.

Fig. 2B shows representative radio chromatogram of urine collected 0-15 h after [^{14}C]-ticlopidine administration. One of the main peaks, metabolite U1, with an RT of 10.1 min, exhibited an $[MH]^+$ ion at m/z 443. The metabolite (RT: 16.4 min) was identified as ticlopidine N-oxide by comparison with an authentic standard. Unchanged ticlopidine was detected at an RT of 31.5 min.

Quantitation of biliary and urinary metabolites. Metabolites were quantified by integration of the peaks of radioactivity found during the radio-HPLC analysis.

During the 0-15 h period after administration, biliary excretion of metabolite B1 represented 15.4% of the dose given, metabolite B2 represented 12.5% of the dose given, and the N-oxide represented 5.2% of the dose given (Fig. 3A). Also, during the 0-15 h period after administration, urinary excretion

of metabolite U1 represented 1.1% of the dose given, the N-oxide represented 1.0% of the dose given, and less than 0.1% of the dose was detected as ticlopidine (Fig. 3B).

Identification of the main biliary metabolite of ticlopidine. The MS spectrum of isolated metabolite B1 exhibited $[MH]^+$ ions at m/z 587 and m/z 589 (Fig. 4A), which represents the ^{35}Cl and ^{37}Cl isotopes. The MS/MS analysis showed a fragment ion at m/z 539 $[MH-SO]^+$ representing the elimination of sulfoxide, 458 $[MH-129]^+$ resulting from neutral loss of pyroglutamate, 410 $[MH-SO-129]^+$, and 280 $[MH-(GSH-S)]^+$ due to cleavage between cysteinyl C-S bond (Fig. 4B), suggesting that metabolite B1 includes a sulfoxide function and GSH moiety.

The ^1H NMR spectrum of isolated metabolite B1 (Fig. 5) consisted of the expected signals for the GSH moiety ($H_{\alpha\text{-Cys}}$, $H_{\alpha\text{-Glu}}$, $H_{\alpha\text{-Gly}}$, $H_{\beta\text{-Cys}}$, $H_{\gamma\text{-Glu}}$, and $H_{\beta\text{-Glu}}$). The ^1H-^1H COSY NMR spectrum (Fig. 5) showed the marked correlation between the H_3 signal at 6.21 ppm and the $H_{2\beta}$ signal at 3.60 ppm. Another correlation between the H_3 signal and the $H_{2\alpha}$ signal at 4.30 ppm was also observed. The two signals of $H_{2\beta}$ and $H_{2\alpha}$ were assigned by a correlation in the COSY spectrum and their characteristic geminal coupling constant of 18 Hz. The ^{13}C-NMR spectrum of B1 (Fig. 6) showed the expected signals for the GSH moiety ($C_{\alpha\text{-Glu}}$, $C_{\alpha\text{-Cys}}$, $C_{\alpha\text{-Gly}}$, $C_{\gamma\text{-Glu}}$, $C_{\beta\text{-Cys}}$, and $C_{\beta\text{-Glu}}$). Complete proton and carbon chemical shift assignments were accomplished using the ^1H-^1H COSY and ^1H-^{13}C COSY NMR spectra. These MS, ^1H-NMR, and ^{13}C-NMR data on metabolite B1 strongly indicated that GSH was conjugated at the carbon 7a of the S-oxide. (The systematic nomenclature for this novel metabolite B1: 2-Amino-4-{1-(carboxymethyl-carbamoyl)-2-[5-(2-chloro-benzyl)-1-oxo-1,2,4,5,6,7-hexahydro-1lambda*4*-thieno[3,2-c]pyridin-7a-ylsulfanyl]-ethylcarbamoyl}-butyric acid.)

The product ion spectrum of metabolite B2 (Fig. 7) included ions at m/z 569 $[MH-H_2O]^+$, 458 $[MH-129]^+$, and 280 $[MH-(GSH-S)]^+$ as observed in that of metabolite B1. On the other hand, its spectrum pattern was slightly different from that of metabolite B1, for example, the relative intensity of the fragment ion at m/z 539 (possible loss of sulfoxide) was weaker than m/z 569 (loss of water) while m/z 539 was major and m/z 569 was minor in the spectrum of metabolite B1. From the present data

available, metabolite B2 is thought to be a GSH conjugate but the substituent positions of GSH and oxygen within the thiophene ring could not be definitely determined.

The product ion spectrum of U1 (having an $[MH]^+$ ion at m/z 443) exhibited a major daughter ion at 395 $[MH-SO]^+$, representing a loss of sulfoxide, and also had minor ions at 425 $[MH-H_2O]^+$ due to loss of water and 280 $[MH-(N\text{-acetylcystein-S})]^+$ attributed to cleavage in the cysteinyl C-S bond. A GSH conjugate loses glycine and glutamic acid to yield the cysteine conjugate, which is acetylated to mercapturic acid (Boyland and Chasseaud, 1969). Therefore, urinary metabolite U1 is thought to be mercapturic acid derived from the GSH conjugates detected in bile. The product ion spectra of U1 and B1 commonly showed major daughter ions at $[MH-SO]^+$, which was not observed in the spectrum pattern of metabolite B2, where the ion at $[MH-H_2O]^+$ was favored over the minor ion at $[MH-SO]^+$. Accordingly, metabolite U1 would be generated from metabolite B1 rather than from metabolite B2, through physiological translation to N-acetylcystein conjugate (Fig. 8).

In vitro metabolism of ticlopidine. Fig. 9 shows HPLC/UV chromatogram from the incubation of ticlopidine with rat liver S9 for 120 min. In addition to the unchanged ticlopidine (RT: 26.5 min), several metabolites were formed. Two metabolites (RT: 9.9 min and 11.2 min), which yielded an $[MH]^+$ ion at m/z 587, were assigned as GSH conjugates corresponding to metabolite B1 and metabolite B2 found in rat bile, respectively. The metabolites (RT: 14.2 min and 21.9 min) were identified as ticlopidine N-oxide and 2-oxo ticlopidine, respectively, by comparison with authentic standard substances. The metabolites (RT: 20.2 and 20.9 min), exhibiting $[MH]^+$ ions at m/z 278 and 280 (data not shown), were the lactam forms of ticlopidine and hydroxyticlopidine, respectively, as described previously (Dalvie and O'Connell, 2004). The peak of M1 at an RT of 18.8 min was an unknown metabolite. The peak at an RT of 22.4 min was assigned as ticlopidine S-oxide dimer (TSOD) after complete purification followed by MS and NMR analyses, the formation of which has been already reported (Ha-Duong et al., 2001).

Identification of in vitro metabolite of ticlopidine. In the MS spectrum of the isolated M1 (Fig. 10A), ions $[MH]^+$ at m/z 296 and m/z 298, representing the ^{35}Cl and ^{37}Cl isotopes, were observed. The product ion spectrum implied that M1 contains carboxylic acid and a thioketone group (Fig. 10B).

Fig. 11 shows the ^1H-^1H COSY NMR spectrum of the metabolite M1. Signals corresponding to the benzene ring protons (H_{Ph3}-H_{Ph6}) were found at 7.24-7.49 ppm for 4 protons. Each proton assignment on the piperidine ring was conducted based on the correlation pattern in the COSY spectrum. The signal for one of the methylene protons at 3.27-3.34 ppm seems to be overlapped with the signal derived from deuterium methanol. This was supported by a correlation between the signal at 3.27-3.34 ppm and the signal for another methylene proton at 3.69 ppm in the spectrum. A signal characteristic of benzyl protons was also observed at 3.79-3.80 ppm. A singlet corresponding to the olefin proton was observed at 5.96 ppm, suggesting that metabolism had occurred at the thiophene ring of ticlopidine.

From the evidence provided by the MS and NMR spectra, the chemical structure of M1 was assigned as a thiophene ring-opened thioketone metabolite (ROT: [1-(2-Chloro-benzyl)-4-thioxo-piperidin-(3Z)-ylidene]-acetic acid in systematic nomenclature).

In vitro metabolism of 2-oxo ticlopidine. In order to elucidate the metabolic route on the pharmacologically active metabolite responsible for anti-platelet activity, another in vitro oxidation was performed using rat liver microsomes. In this oxidation, 2-oxo ticlopidine was used as a substrate in order to produce an amount of the active form sufficient for detection. Fig. 12 shows reconstructed ion ($[MH]^+$ at m/z 298) and UV chromatograms from incubation of 2-oxo ticlopidine with rat liver microsomes for 60 min. The production of the pharmacologically active metabolite (RT: 13.1 min) was confirmed by co-chromatography (chromatographic analysis of that incubation spiked with an authentic standard). ROT was also detected as a metabolite of 2-oxo ticlopidine (Fig. 12).

Discussion

We studied the metabolism of ticlopidine in rats and identified two GSH conjugates of ticlopidine (B1 and B2) in bile and mercapturate in urine (U1) after the administration of ticlopidine. One of the

GSH conjugates (B1) was isolated and its structure was completely characterized as a GSH conjugate of S-oxide, in which conjugation had occurred at carbon 7a in the thienopyridine moiety. It has been reported that thiophene compounds such as tienilic acid and thiophene itself form highly reactive S-oxide during hepatic metabolism, which are either trapped by GSH and eventually excreted in urine as mercapturate (Dansette et al., 1992, Valadon et al., 1996) or irreversibly bind to macromolecules such as hepatic microsomal proteins (Koenigs et al., 1999, López-Garcia et al., 1994). Ha-Duong reported the generation of ticlopidine S-oxide dimmer derived from the Diels-Alder type dimerization of this reactive S-oxide in vitro (Ha-Duong et al., 2001). These reports are completely in agreement with our findings on the in vivo metabolites of ticlopidine, in which the structure contains a thiophene moiety.

The location of the glutathionyl moiety in the GSH conjugate of S-oxide (B1) was determined to be carbon 7a position in thienopyridine moiety by MS/MS and NMR analysis. As shown in Fig. 4, the product ion spectrum suggests that B1 contains a sulfoxide function and a GSH moiety. As illustrated in Fig. 5, the H_3 signal was coupled with two geminal proton signals of $H_{2\beta}$ and $H_{2\alpha}$. These MS/MS and NMR data can only be explained by the attachment of GSH at carbon 7a of ticlopidine S-oxide. In our ^{1}H NMR spectrum, the H_3 signal was broadened, although it could be spirited by the adjacent $H_{2\beta}$ and $H_{2\alpha}$. However, the corresponding proton signal at the dihydrothiophene ring was also broadened in the ^{1}H NMR spectrum of the mercaptoethanol adduct of the thiophene S-oxide, where the $S(CH_2)_2OH$ group is substituted at the corresponding carbon adjacent to the sulfoxide function (Valadon et al, 1996). Although we could not definitely characterize the incorporated position of GSH and oxygen at the thiophene ring, another GSH conjugate (B2, isomer of B1) was also detected. Dansette reported interesting MS/MS fragment analyses on the two GSH conjugates of 2-phenylthiophene, where the loss of 48 amu (sulfoxide) was favored over the loss of 18 amu (water) in the case of GSH conjugate of the thiophene-S-oxide, whereas the loss of 18 amu was dominant in the case of 5-hydroxy-4-glutathionyl-4,5dihydrothiophene resulting from the addition of GSH to the thiophene epoxide (Dansette et al., 2005). However, another thiophene GSH adduct of S-oxide showed no loss of 48 amu, but did show a loss of 18 amu in the product ion spectrum (Medower et al., 2008). Recently, GSH adducts derived

from both thiophene-S-oxide and thiophene epoxide were identified in the microsomal incubation of 2-phenylthiophene, demonstrating that thiophene derivatives could simultaneously afford two intermediates, S-oxide and epoxide, during hepatic metabolism (Dansette et al., 2005). Therefore, B2 could be generated by the addition of GSH to either a thiophene S-oxide or a thiophene epoxide. Further structural analyses, including an NMR study, are necessary to determine the substituted positions of GSH and oxygen in B2.

During the first 15 h after administration, the total amount of the GSH conjugates and mercapturic acid was 29% of the administered dose (Fig. 3A and 3B). This is the first report that quantitatively reveals the metabolic activation (including both S-oxidation and putative epoxydation) of ticlopidine in vivo. N-oxide found in rat bile and urine was a total of 6% of the dose in our study (Fig. 3A and 3B). Tuong reported that 16% of administered ticlopidine was excreted in rat urine as N-dealkylated metabolites (Tuong et al, 1981). These observations indicate that the formations of reactive intermediates followed by conjugation with GSH are the major metabolic routes of ticlopidine in rats. Ticlopidine has been reported to induce agranulocytosis (Ono et al., 1991), thrombotic thrombocytopenic purpura (Muzkat et al., 1998; Steinhubl et al., 1999), aplastic anemia (Mataix et al., 1992; Ferrer et al., 1998), and hepatotoxicity (Takikawa, 2005). Immune reactions seem to be involved in at least some serious adverse events, such as agranulocytosis (Ono et al., 1991) and hepatic injury (Zanten et al., 1996; Tsai MH et al., 2000). Recently, it has been suggested that reactive metabolites followed by covalent binding are associated with idiosyncratic toxicity through immune mechanisms. Thus, although additional studies are needed to clarify the metabolic pathways of ticlopidine in humans, our quantitative analyses on metabolic activation pathways in rats could support the hypothesis that reactive metabolites such as S-oxide are responsible for ticlopidine-induced adverse events in humans.

Incubation of ticlopidine with rat liver S9 resulted in several products including known metabolites (N-oxide, Lactam form, hydroxylated form, TSOD, and 2-oxo ticlopidine) and novel metabolites (GSH conjugates and ROT, Fig. 9). TSOD was detected in vitro but not in vivo while GSH conjugate(s) of the reactive S-oxide were formed both in vitro and in vivo. It is presumably because the concentration of

the S-oxide formed in vitro is high enough to dimerize. In contrast, the concentration in vivo is too low for an S-oxide molecule to access another one and results in conjugation with hepatic GSH. The pharmacologically active metabolite was generated by incubation of 2-oxo ticlopidine with rat liver microsomes (Fig. 12) as reported previously (Yoneda et al., 2004). ROT, a novel thiophene-ring opened metabolite with a thioketone group and a carboxylic function, was also found during in vitro oxidation from 2-oxo ticlopidine (Fig. 12) as well as from ticlopidine itself (Fig. 9) and this metabolite is likely to be formed by oxidation at the thiol group of the pharmacologically active metabolite.

From the results of the present in vivo and in vitro studies, the metabolic pathways of ticlopidine are postulated as depicted in Fig. 13. Oxidation of the thiophene sulfur atom yields a reactive S-oxide, which undergoes either dimerization to form TSOD or a reaction with GSH to give GSH conjugate(s). The resulting GSH conjugate loses glycine and glutamic acid to yield a cysteine conjugate that is acetylated to the corresponding mercapturic acid. An alternative putative oxidative activation route is epoxidation which can also afford GSH conjugate. The total amount of GSH conjugates and mercapturic acid was 29% of the administered dose, which demonstrates that the activation pathways are the major in vivo metabolic routes of ticlopidine in rats. The other main routes appear to be N-dealkylation and N-oxidation. Lactam and hydroxylated metabolites were also detected in vitro. An S-oxide intermediate could also undergo a rearrangement to 2-oxo ticlopidine, although it is possible for epoxide intermediate to yield 2-oxo ticlopidine through the nucleophilic addition of water followed by dehydration (Ha-Duong et al., 2001). This 2-oxo form is biotransformed into the pharmacologically active metabolite of ticlopidine responsible for platelet inhibition. The resulting active metabolite is further oxidized at the thiol group to yield ROT.

In conclusion, we have identified several novel metabolites and revealed the metabolic pathways of ticlopdine. The main biliary metabolite of ticlopidine was the GSH conjugate of S-oxide, in which conjugation had occurred at the carbon 7a in the thienopyridine moiety. Furthermore, 29% of the administered ticlopidine was subjected to the formation of reactive intermediates followed by conjugation with GSH in vivo in rats. In vitro incubation of ticlopidine with rat liver S9 fractions led to

DMD Fast Forward. Published on June 18, 2009 as DOI: 10.1124/dmd.109.027524

the formation of multiple metabolites, including 2-oxo-ticlopidine, the precursor for the pharmacologically active ticlopidine metabolite. A novel thiophene-ring opened metabolite with a thioketone group and a carboxylic acid moiety has also been detected after incubation of 2-oxo-ticlopidine with rat liver microsomes or upon incubation of ticlopidine with rat liver S9 fractions.

References.

Belghazi M, Jean P, Poli S, Schmitter JM, Mansuy D, Dansette PM (2001) Use of isotopes and LC-MS-ESI-TOF for mechanistic studies of tienilic acid metabolic activation. Adv Exp Med Biol 500: 139-44.

Boyland E, Chasseaud LF (1969) The role of glutathione and glutathione S-transferases in mercapturic acid biosynthesis. *Adv Enzymol Relat Areas Mol Biol* **32:** 173-219.

Dalvie DK, O'Connell TN (2004) Characterization of novel dihydrothienopyridinium and thienopyridinium metabolites of ticlopidine in vitro: role of peroxidases, cytochromes p450, and monoamine oxidases. *Drug Metab Dispos* **32:** 49-57.

Dansette PM, Bertho G, Mansuy D (2005) First evidence that cytochrome P450 may catalyze both S-oxidation and epoxidation of thiophene derivatives. *Biochem Biophys Res Commun* **338:** 450-5.

Dansette PM, Thang DC, el Amri H, Mansuy D (1992) Evidence for thiophene-S-oxide as a primary reactive metabolite of thiophene in vivo: formation of a dihydrothiophene sulfoxide mercapturic acid. *Biochem Biophys Res Commun* **186:** 1624-30.

Ferrer F, De Arriba F, Moraleda, JM, and Vicente V (1998) Aplastic Anaemia Induced by Ticlopidine after Placement of Coronary Artery Stents: Therapeutic Role of Granulocyte Colony-Stimulating Factor. *Clin. Drug. Investig* **15:** 261-262.

Ha-Duong NT, Dijols S, Macherey AC, Goldstein JA, Dansette PM, Mansuy D (2001) Ticlopidine as a selective mechanism-based inhibitor of human cytochrome P450 2C19. *Biochemistry* **40:** 12112-22.

Ito T, Takahashi M, Sudo K, Sugiyama Y. (2007) Marked strain differences in the pharmacokinetics of an alpha4beta1 integrin antagonist, 4-[1-[3-Chloro-4-[N-(2-methylphenyl)-ureido]phenylacetyl]-

(4S)-fluoro-(2S)-pyrrolidine-2-yl]-methoxybenzoic Acid (D01-4582), in Sprague-Dawley rats are associated with albumin genetic polymorphism. *J Pharmacol Exp Ther.* **320:**124-32

Jacobson AK (2004) Platelet ADP receptor antagonists: ticlopidine and clopidogrel. *Best Pract Res Clin Haematol* **17:** 55-64.

Koenigs LL, Peter RM, Hunter AP, Haining RL, Rettie AE, Friedberg T, Pritchard MP, Shou M, Rushmore TH, Trager WF (1999) Electrospray ionization mass spectrometric analysis of intact cytochrome P450: identification of tienilic acid adducts to P450 2C9. *Biochemistry* **38:** 2312-9.

López-Garcia MP, Dansette PM, Mansuy D (1994) Thiophene derivatives as new mechanism-based inhibitors of cytochromes P-450: inactivation of yeast-expressed human liver cytochrome P-450 2C9 by tienilic acid. *Biochemistry* **33:**166-75.

Mataix R, Ojeda E, Perez MC, Jimenez S (1992) Ticlopidine and severe aplastic anaemia. *Br J Haemato.* **80:** 125-6.

Medower C, Wen L, Johnson WW (2008) Cytochrome P450 oxidation of the thiophene-containing anticancer drug 3-[(quinolin-4-ylmethyl)-amino]-thiophene-2-carboxylic acid (4-trifluoromethoxy-phenyl)-amide to an electrophilic intermediate. *Chem Res Toxicol* **21:** 1570-7.

Muszkat M, Shapira MY, Sviri S, Linton DM, Caraco Y (1998) Ticlopidine-induced thrombotic thrombocytopenic purpura. *Pharmacotherapy* **18:** 1352-5.

Noble S, Goa KL (1996) Ticlopidine. A review of its pharmacology, clinical efficacy and tolerability in the prevention of cerebral ischaemia and stroke. *Drugs Aging* **8:** 214-32.

Ono K, Kurohara K, Yoshihara M, Shimamoto Y, Yamaguchi M (1991) Agranulocytosis caused by ticlopidine and its mechanism. *Am J Hematol* **37:** 239-42.

Panak E, Maffrand JP, Picard-Fraire C, Vallée E, Blanchard J, Roncucci R (1983) Ticlopidine: a promise for the prevention and treatment of thrombosis and its complications. *Haemostasis* **13 Suppl 1:** 1-54.

Quinn MJ, Fitzgerald DJ (1999) Ticlopidine and clopidogrel. *Circulation* **100:** 1667-72.

Saltiel E, Ward A (1987) Ticlopidine. A review of its pharmacodynamic and pharmacokinetic properties, and therapeutic efficacy in platelet-dependent disease states. *Drugs* **34:** 222-62.

Steinhubl SR, Tan WA, Foody JM, Topol EJ (1999) Incidence and clinical course of thrombotic thrombocytopenic purpura due to ticlopidine following coronary stenting. EPISTENT Investigators. Evaluation of Platelet IIb/IIIa Inhibitor for Stenting. *JAMA* **281:** 806-10.

Takikawa H (2005) Lessons from ticlopidine-induced liver injury. *Hepatol Res* **33:** 193-4.

Tsai MH, Tsai SL, Chen TC, Liaw YF (2000) Ticlopidine-induced cholestatic hepatitis with anti-nuclear antibody in serum. *J Formos Med Assoc* **99:** 866-9.

Tuong A, Bouyssou A, Paret J, Cuong TG (1981) Metabolism of ticlopidine in rats: identification and quantitative determination of some its metabolites in plasma, urine and bile. *Eur J Drug Metab Pharmacokinet* **6:** 91-8.

Valadon P, Dansette PM, Girault JP, Amar C, Mansuy D (1996) Thiophene sulfoxides as reactive metabolites: formation upon microsomal oxidation of a 3-aroylthiophene and fate in the presence of nucleophiles in vitro and in vivo. *Chem Res Toxicol* **9:** 1403-13.

Veldhuyzen van Zanten, McCormic CW (1996) Antinuclear antibody-positive ticlopine-induced hepatitis. *Can J Gastroenterol* **10:** 231-232.

Yoneda K, Iwamura R, Kishi H, Mizukami Y, Mogami K, Kobayashi S (2004) Identification of the active metabolite of ticlopidine from rat in vitro metabolites. *Br J Pharmacol* **142:** 551-7.

DMD Fast Forward. Published on June 18, 2009 as DOI: 10.1124/dmd.109.027524
This article has not been copyedited and formatted. The final version may differ from this version.

Legends for Figures

FIG. 1. *Chemical structure of ticlopidine.*

The position of ^{14}C is denoted by the asterisk.

FIG. 2. *Representative radio-HPLC chromatograms of bile (A) and urine (B) collected during 0-15 h after a single oral administration of [^{14}C]-ticlopidine (22 mg/kg) to rats.*

FIG. 3. *Biliary (A) and urinary (B) excretion of ticlopidine metabolites collected during 0-15 h after a single oral administration of [^{14}C]-ticlopidine (22 mg/kg) to Rats.*

Data were expressed as the mean + standard deviation of 9 rats for biliary metabolites and 3 rats for urinary metabolites. (Only 3 rats could be used for the quantification of urinary metabolites because penis tubes to collect urine were detached in 6 out of 9 animals during 0-15h after administration.)

FIG. 4. *MS spectrum of isolated metabolite B1 (A) and its product ion spectrum (B).*

FIG. 5. *^{1}H-^{1}H COSY NMR spectrum of isolated metabolite B1 in D_2O.*

FIG. 6. *^{13}C-NMR spectrum of isolated metabolite B1 in D_2O.*

FIG. 7. *MS spectrum of metabolite B2 (A) and its product ion spectrum (B).*

FIG. 8. *Product ion spectrum of the metabolite U1*.

FIG. 9. *HPLC/UV chromatogram for metabolites from a 120-min incubation of ticlopidine (1 mM) with rat liver S9.*

FIG. 10. *MS spectrum from isolated metabolite M1 (A) and its product ion spectrum (B).*

FIG. 11. *^{1}H-^{1}H COSY NMR spectrum of isolated metabolite M1 in CD_3OD.*

FIG. 12. *HPLC/MS and UV chromatograms for metabolites from a 60-min incubation of 2-oxo ticlopidine (1 mM) with rat liver microsomes.*

The production of pharmacologically active metabolite (RT: 13.1 min) was confirmed by co-chromatography (chromatographic analysis of that incubation spiked with an authentic standard).

FIG. 13. *Proposed metabolic pathways of ticlopidine.*

*: The incorporated positions of GSH and oxygen at the thiophene ring of B2 was not determined.

B2 and 2-oxo ticlopidine could be derived from the epoxide, the S-oxide, or both.

DMD Fast Forward. Published on June 18, 2009 as DOI: 10.1124/dmd.109.027524
This article has not been copyedited and formatted. The final version may differ from this version.

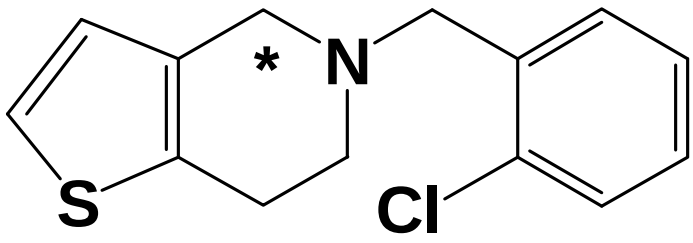

FIG. 1.

DMD Fast Forward. Published on June 18, 2009 as DOI: 10.1124/dmd.109.027524
This article has not been copyedited and formatted. The final version may differ from this version.

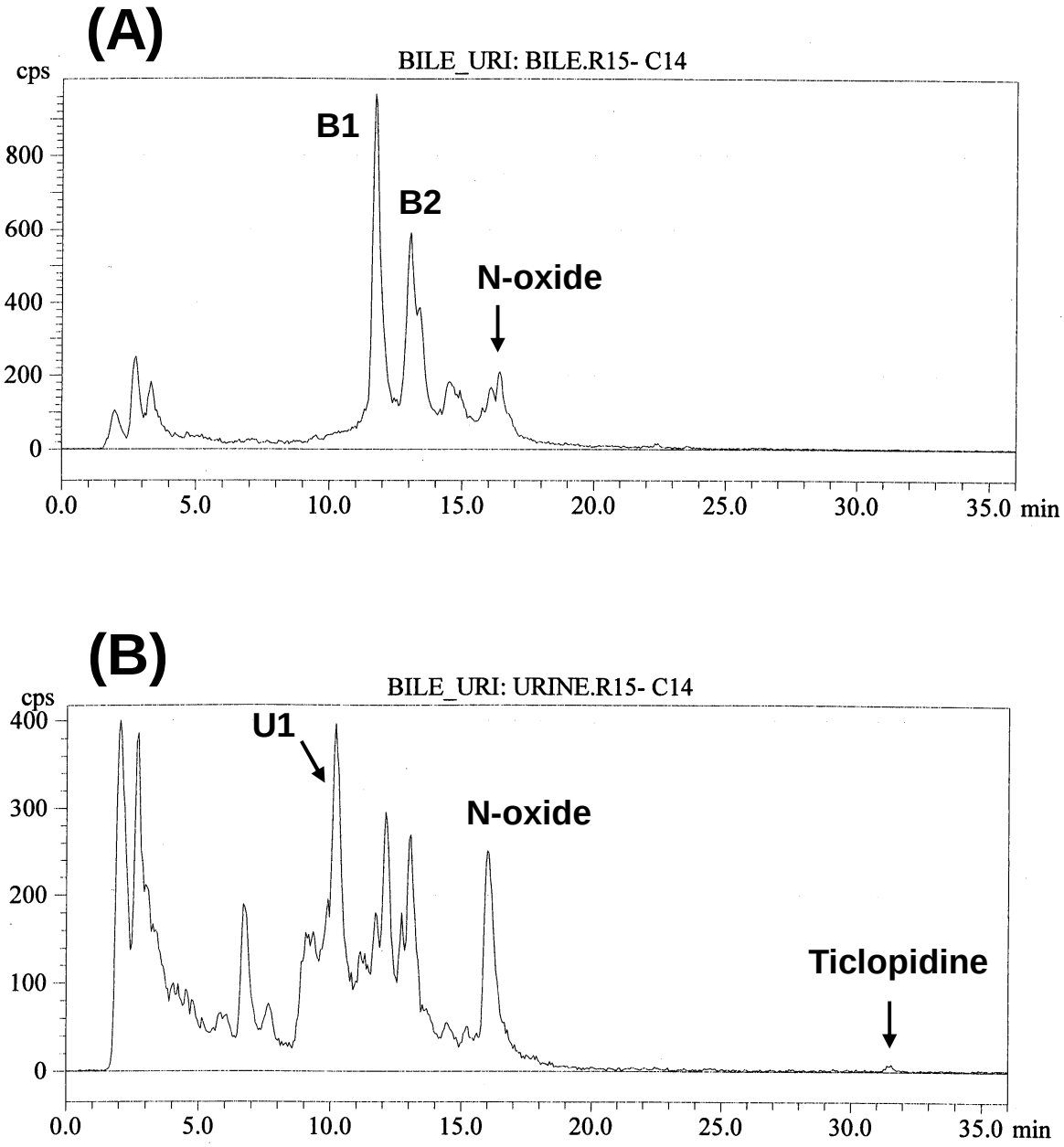

FIG. 2.

DMD Fast Forward. Published on June 18, 2009 as DOI: 10.1124/dmd.109.027524
This article has not been copyedited and formatted. The final version may differ from this version.

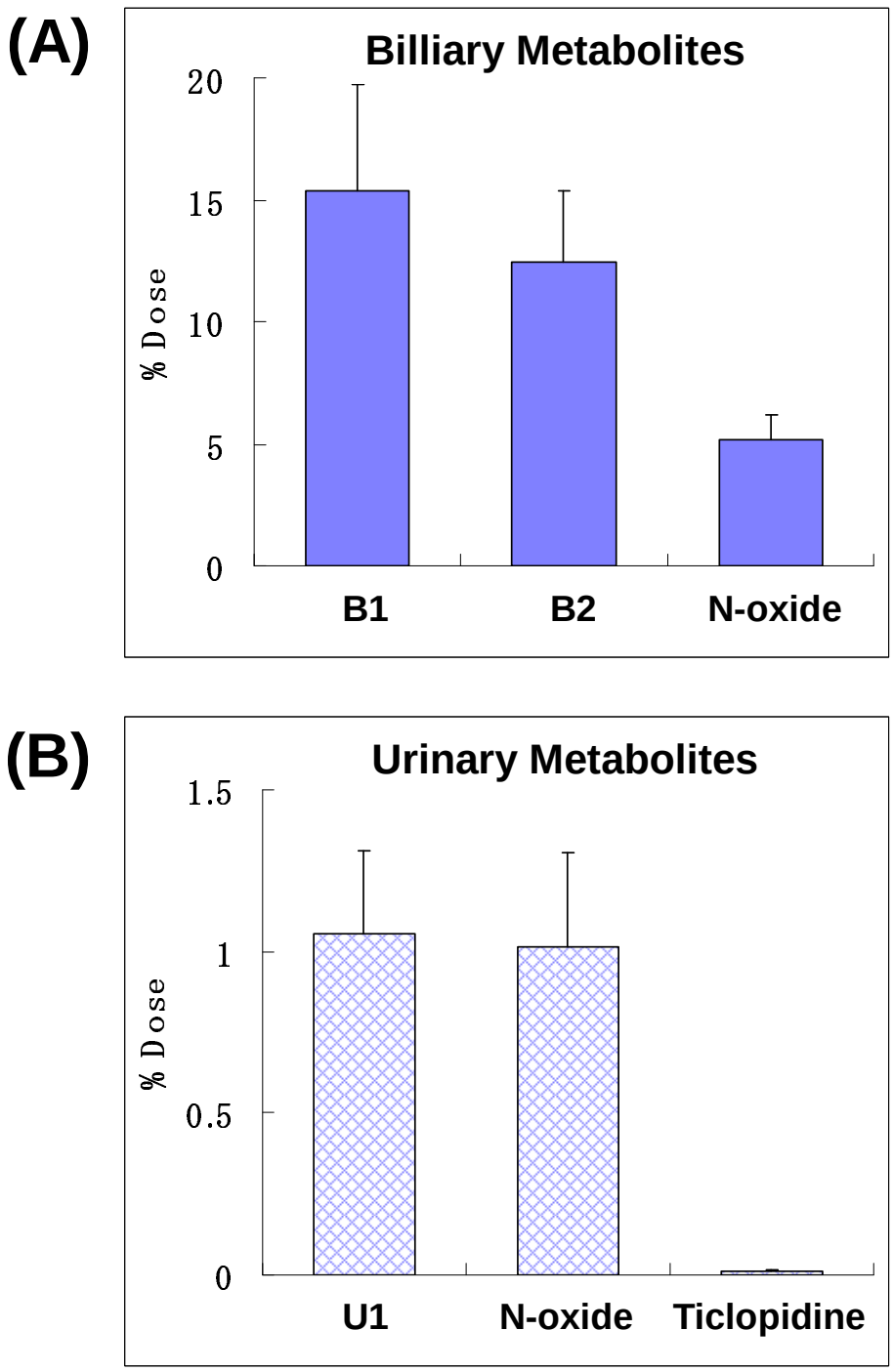

FIG. 3.

DMD Fast Forward. Published on June 18, 2009 as DOI: 10.1124/dmd.109.027524
This article has not been copyedited and formatted. The final version may differ from this version.

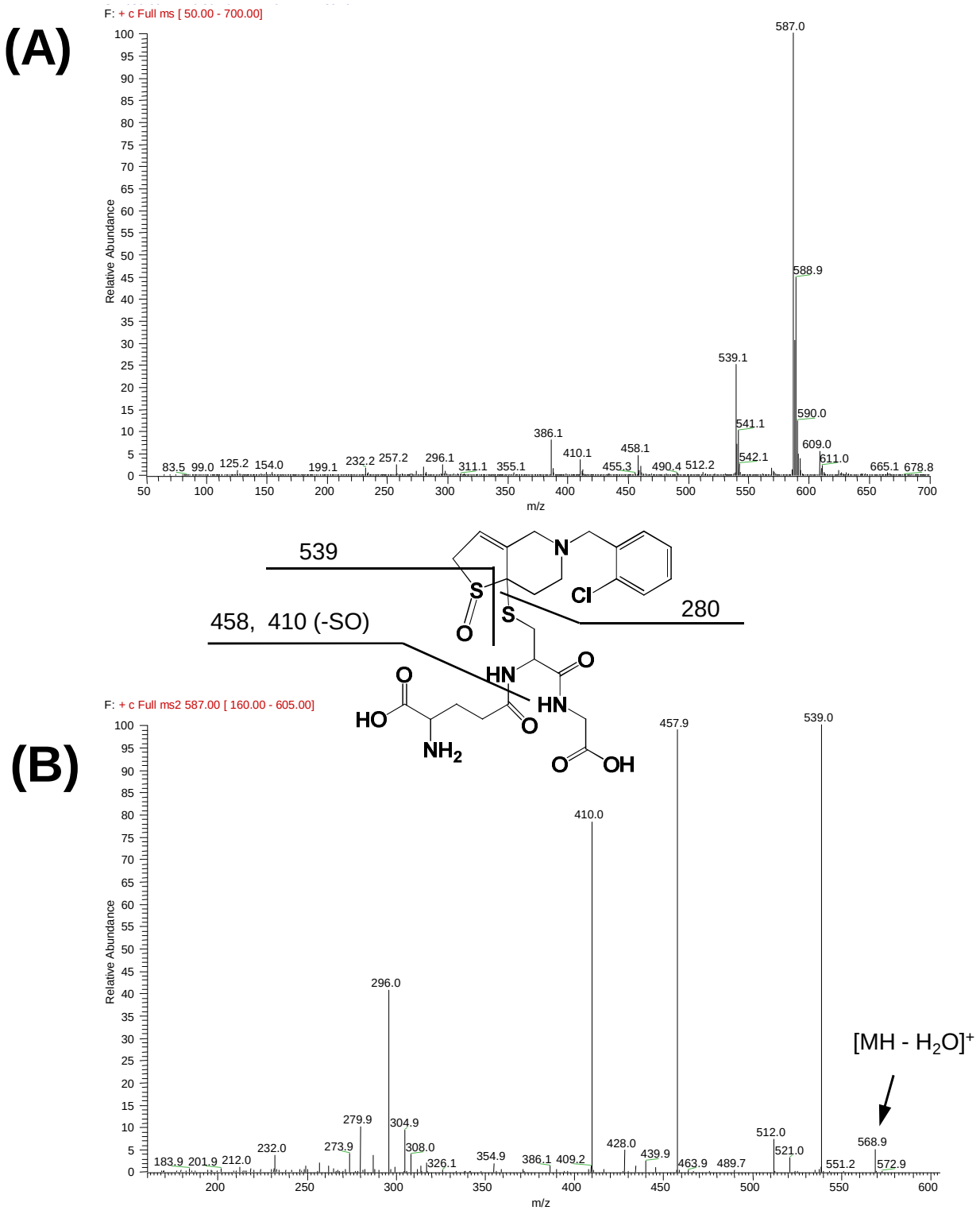

FIG. 4.

DMD Fast Forward. Published on June 18, 2009 as DOI: 10.1124/dmd.109.027524
This article has not been copyedited and formatted. The final version may differ from this version.

Assignment	Chemical Shift (δ in ppm)		J (Hz)		Assignment	Chemical Shift (δ in ppm)		J (Hz)	
2	4.30	d	18	1H	α-Gly	3.73-3.82*			1H
	3.60	d	18	1H	α-Glu	3.73-3.82*			1H
3	6.21	broaden		1H	β-Glu	2.14-2.19	m		2H
4	4.16	d	14	1H	γ-Glu	2.54	t	7	2H
	3.73-3.82*			1H	α-Cys	4.68	dd	5, 8	1H
6	3.51-3.61	m		2H	β-Cys	3.13	dd	8, 14	1H
7	2.59-2.62	m		1H		3.05	dd	5, 14	1H
	2.27	d	15	1H					
Bn	4.35	d	13	1H					
	4.39	d	13	1H					
12-15	7.43-7.60	m		4H					

*: ^{1}H NMR signals of 4β, α-Gly, and α-Glu were overlapped.

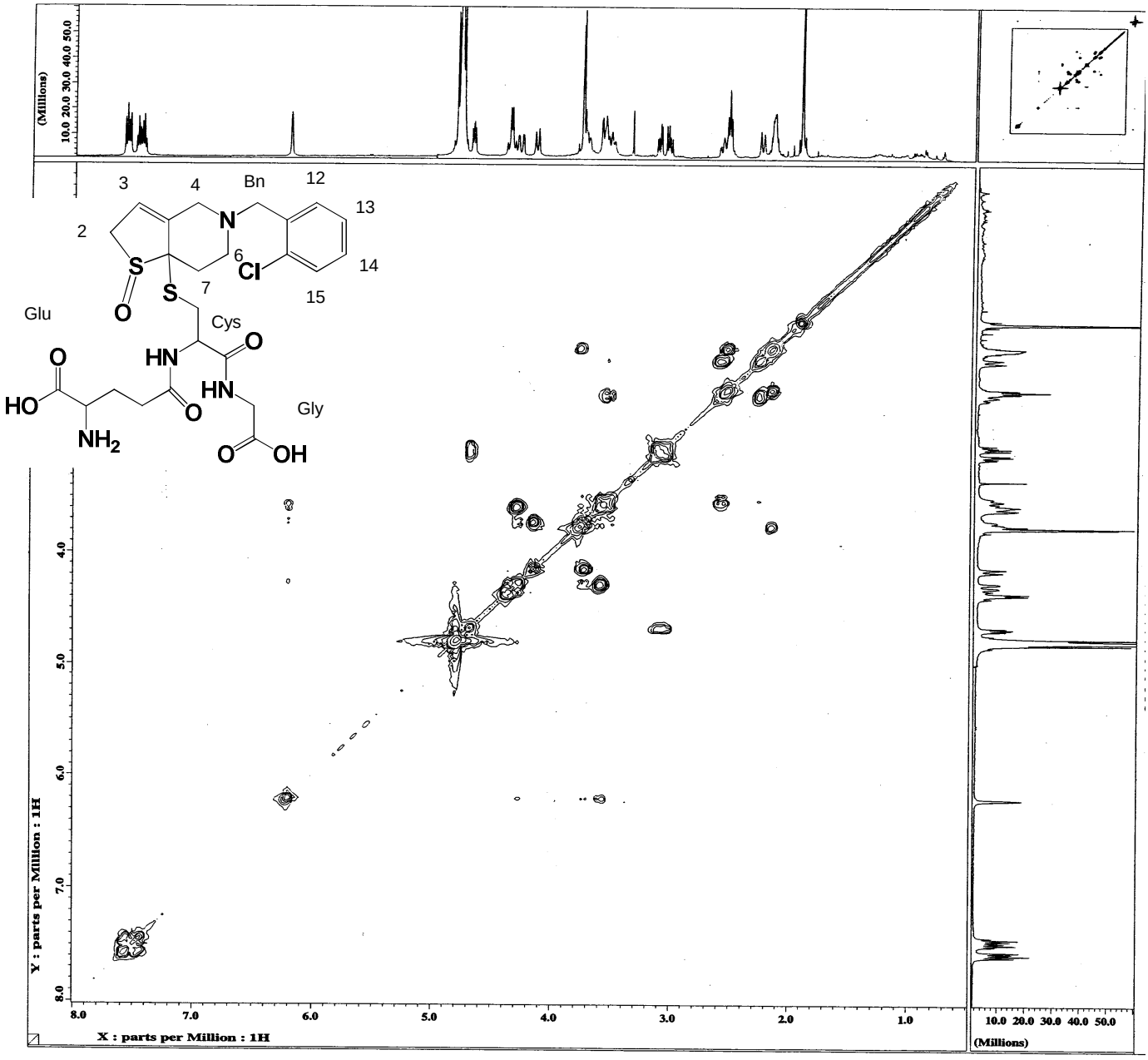

FIG. 5.

DMD Fast Forward. Published on June 18, 2009 as DOI: 10.1124/dmd.109.027524
This article has not been copyedited and formatted. The final version may differ from this version.

Assignment	Chemical Shift (δ in ppm)		Assignment	Chemical Shift (δ in ppm)	
2	59.3 or 59.1	CH_2	α-Gly	46.2	CH
3	130.4	CH	α-Glu	57.0	CH
3a	131.8	Cq	β-Glu	29.1	CH_2
4	53.1	CH_2	γ-Glu	34.3	CH_2
6	49.2	CH_2	α-Cys	55.7	CH
7	24.9	CH_2	β-Cys	34.2	CH_2
7a	79.5	Cq			
Bn	59.3 or 59.1	CH_2			
11	137.9	Cq			
12	134.2 or 133.0	CH			
13	130.5	CH			
14	135.9	CH			
15	134.2 or 133.0	CH			
16	134.5	Cq			

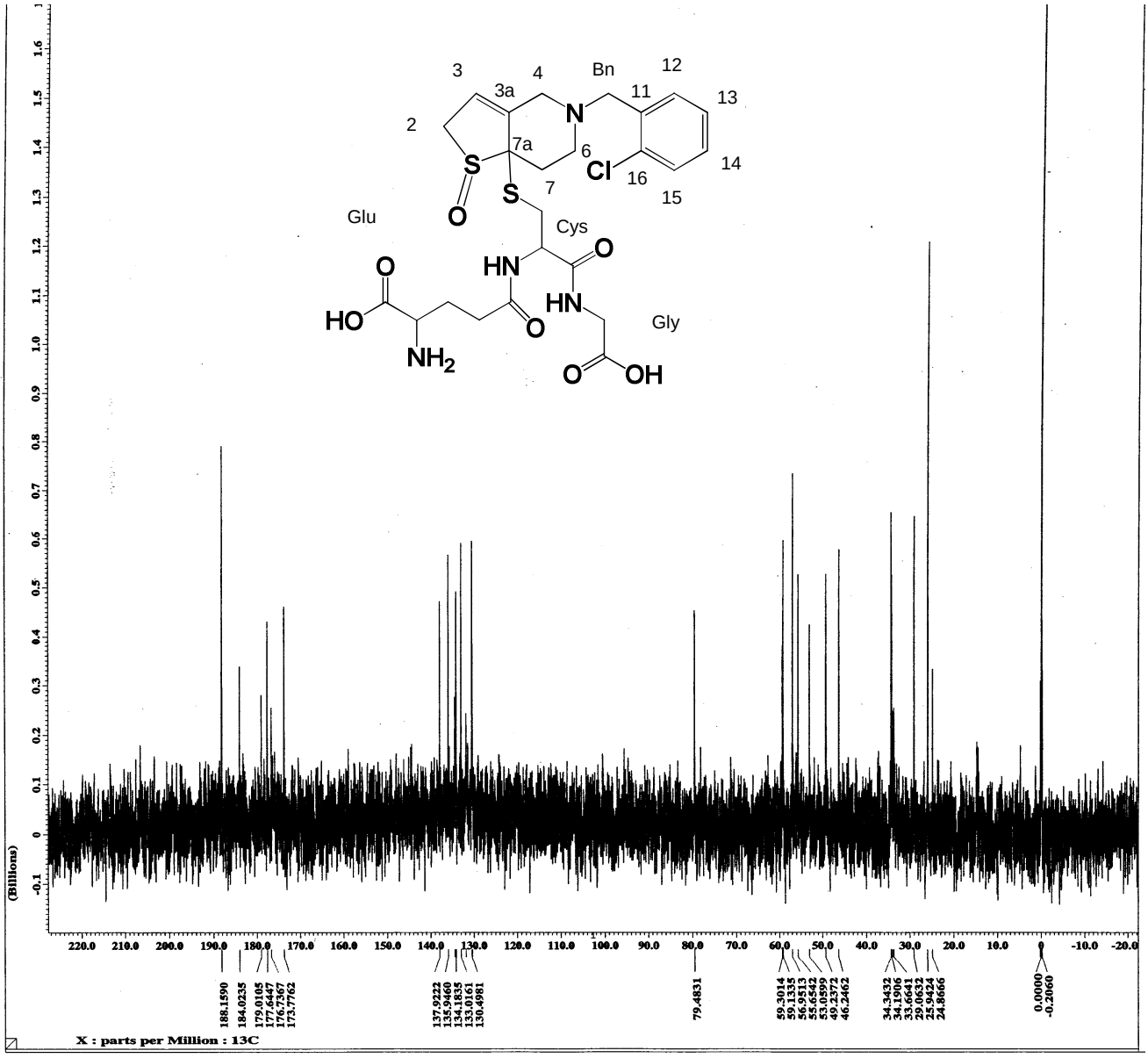

FIG. 6.

DMD Fast Forward. Published on June 18, 2009 as DOI: 10.1124/dmd.109.027524
This article has not been copyedited and formatted. The final version may differ from this version.

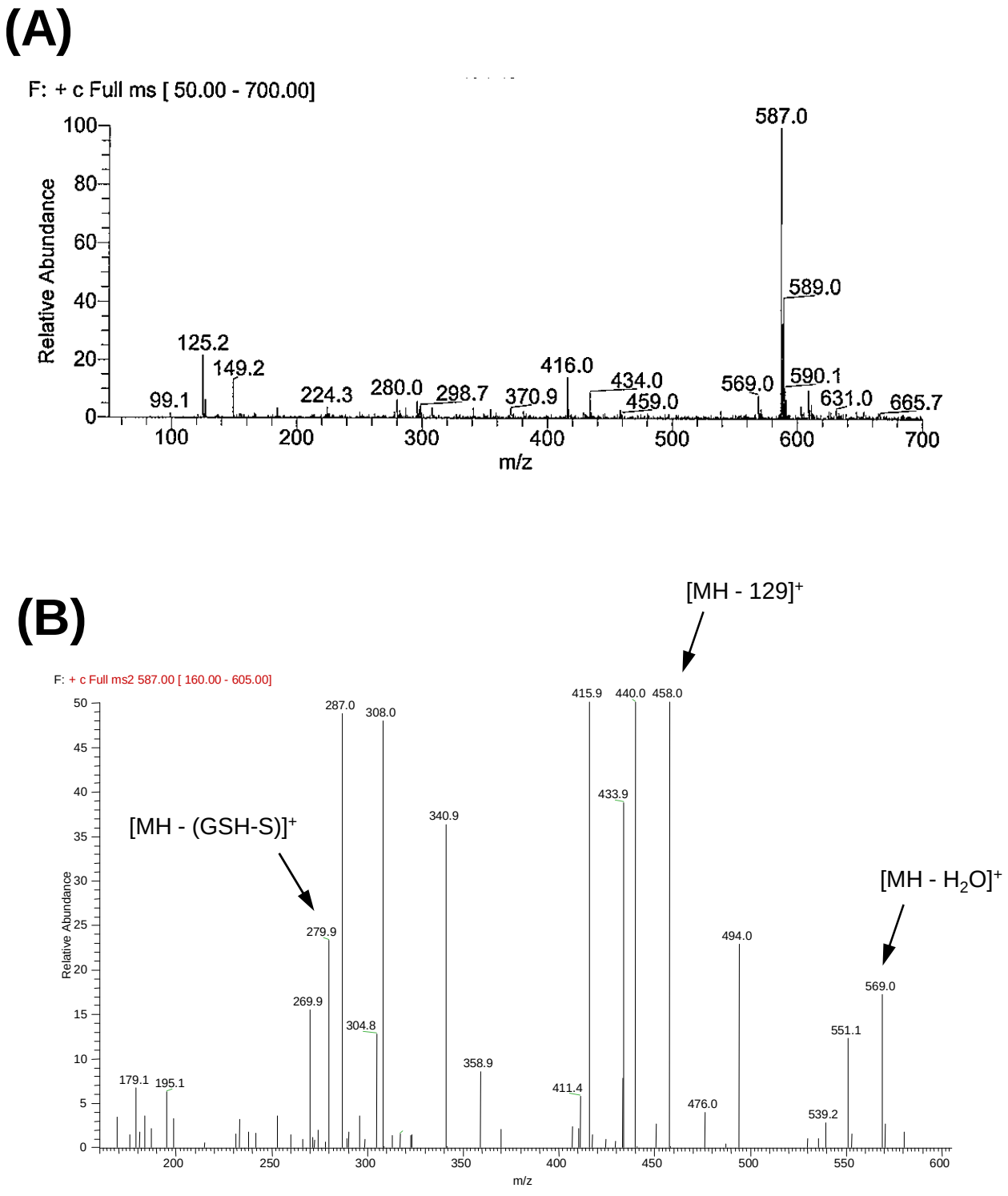

FIG. 7.

DMD Fast Forward. Published on June 18, 2009 as DOI: 10.1124/dmd.109.027524
This article has not been copyedited and formatted. The final version may differ from this version.

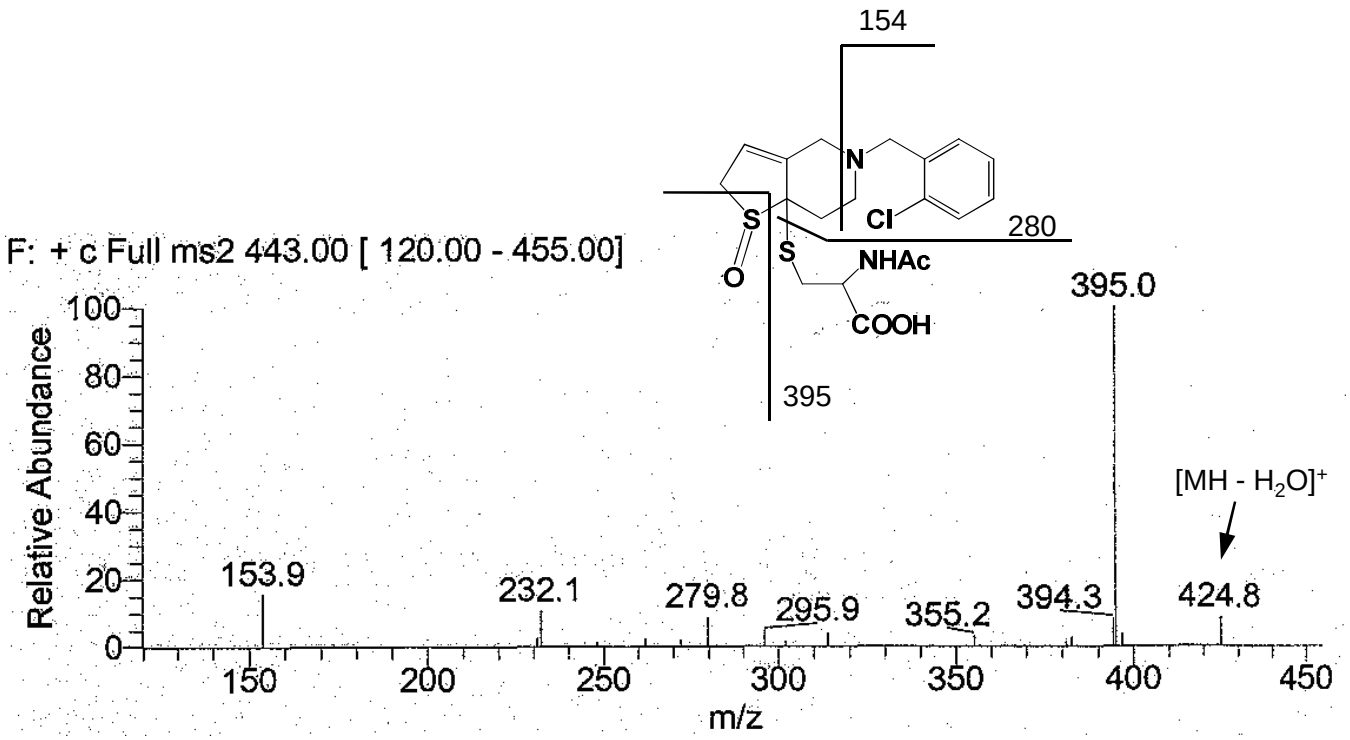

FIG. 8.

DMD Fast Forward. Published on June 18, 2009 as DOI: 10.1124/dmd.109.027524
This article has not been copyedited and formatted. The final version may differ from this version.

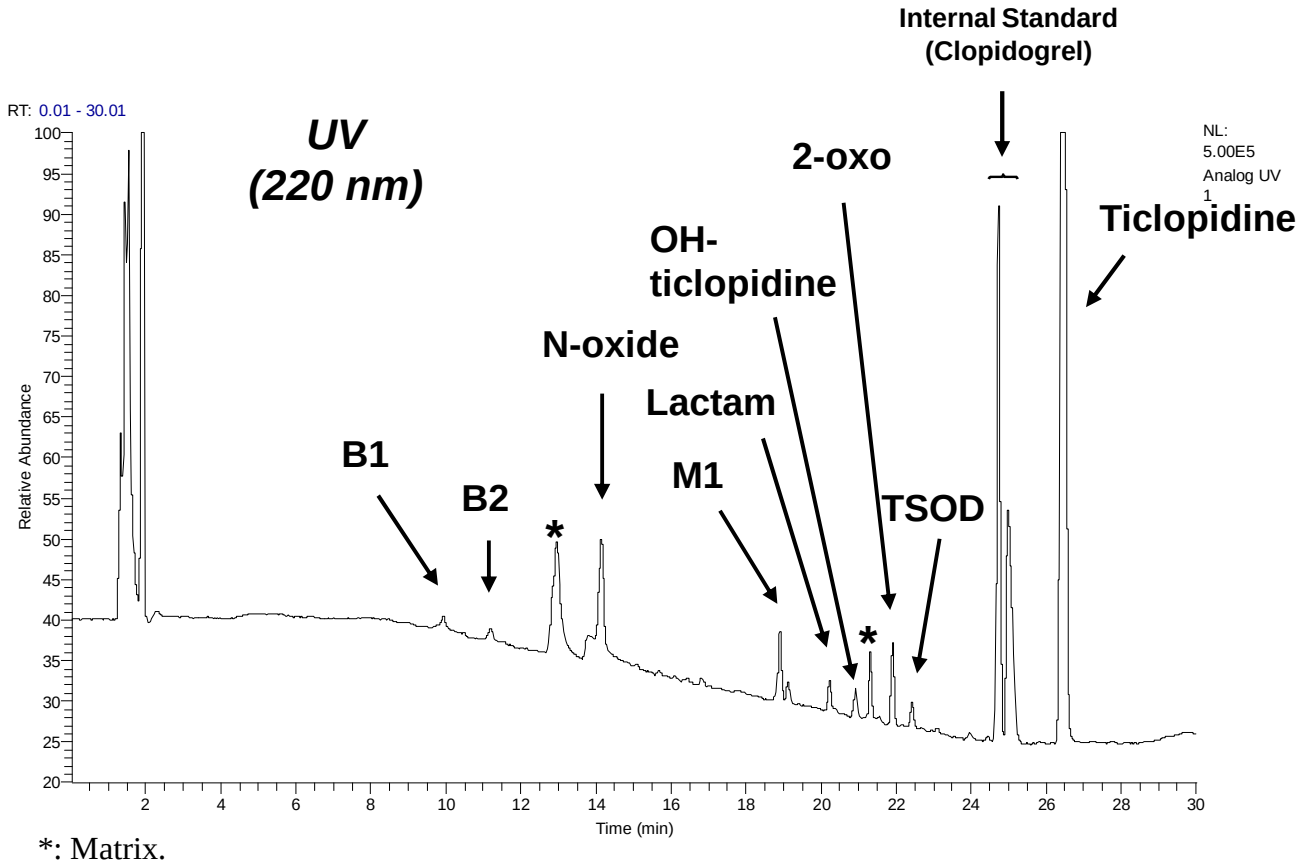

*: Matrix.

FIG. 9.

DMD Fast Forward. Published on June 18, 2009 as DOI: 10.1124/dmd.109.027524
This article has not been copyedited and formatted. The final version may differ from this version.

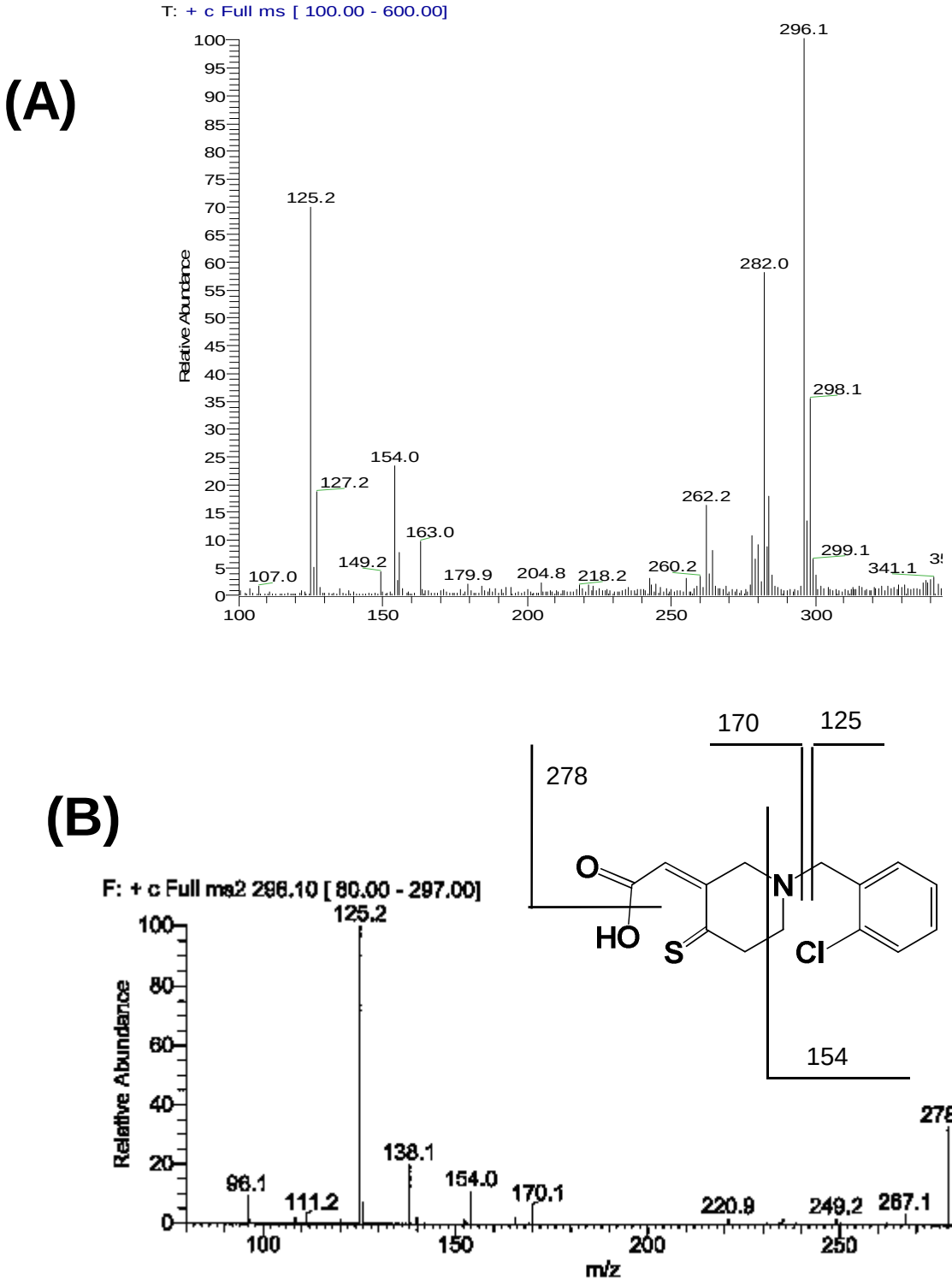

FIG. 10.

DMD Fast Forward. Published on June 18, 2009 as DOI: 10.1124/dmd.109.027524
This article has not been copyedited and formatted. The final version may differ from this version.

Assignment	Chemical shift (δ in ppm)		
2	3.69	d	1H
	3.27-3.34*		1H
5	2.53	d	1H
	2.19-2.26	m	1H
6	2.76-2.81	m	2H
Bn	3.80	s	2H
olefin	5.96	s	1H
Ph,3-6	7.24-7.49	m	4H

*: ^{1}H NMR signal was overlapped with the signal derived from deuterium methanol.

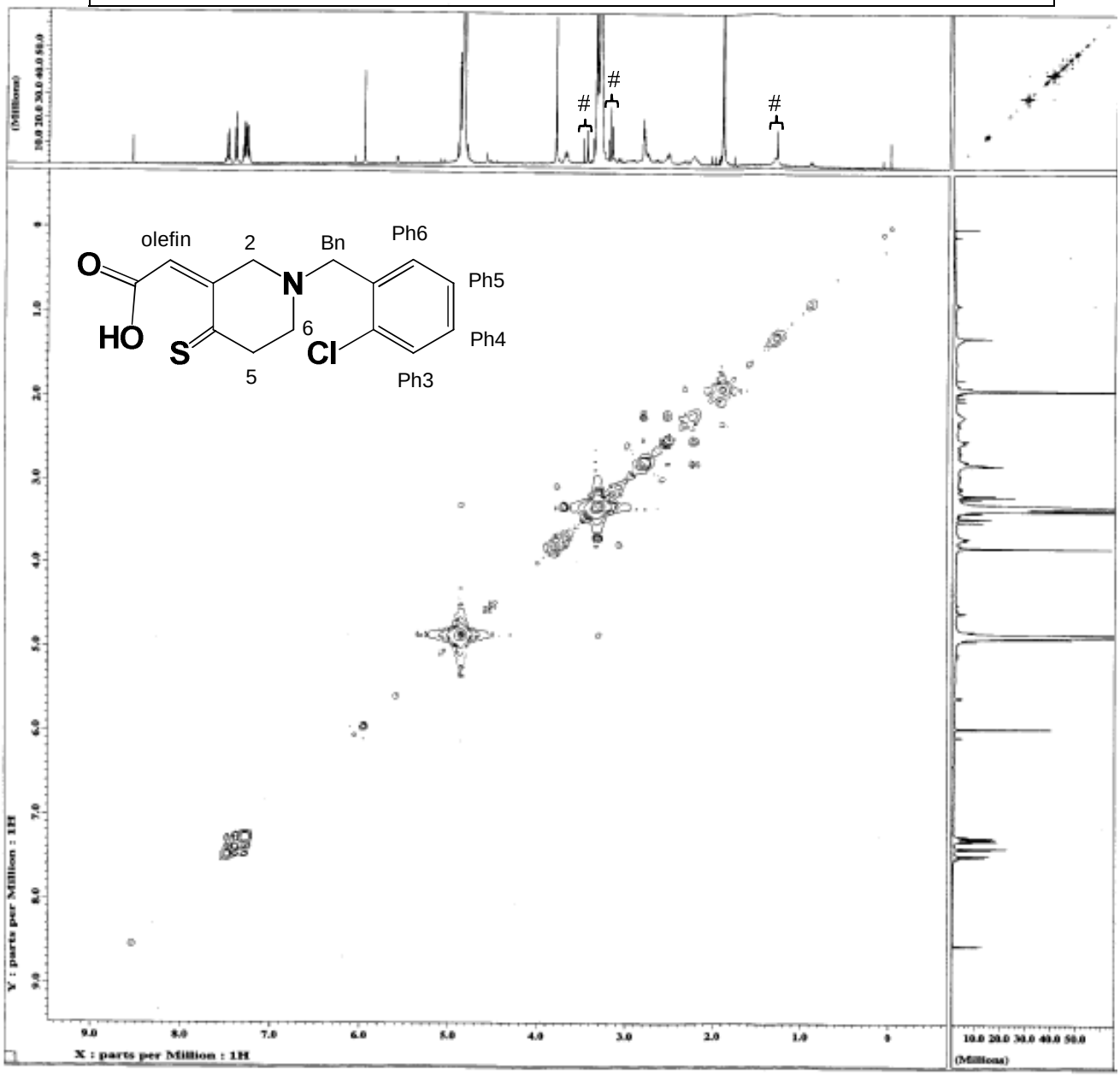

#: Impurity

FIG. 11.

DMD Fast Forward. Published on June 18, 2009 as DOI: 10.1124/dmd.109.027524
This article has not been copyedited and formatted. The final version may differ from this version.

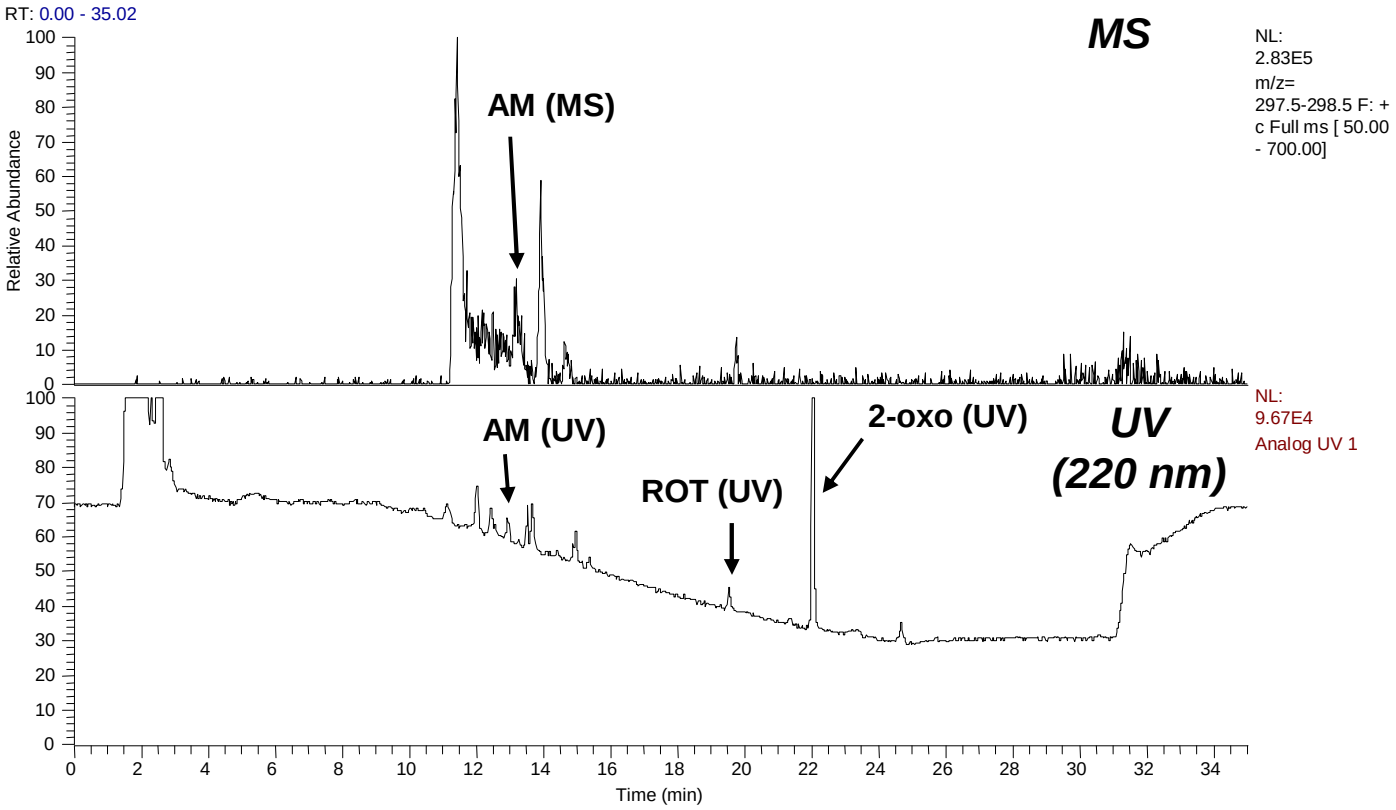

AM: pharmacologically active metabolite

FIG. 12.

DMD Fast Forward. Published on June 18, 2009 as DOI: 10.1124/dmd.109.027524
This article has not been copyedited and formatted. The final version may differ from this version.

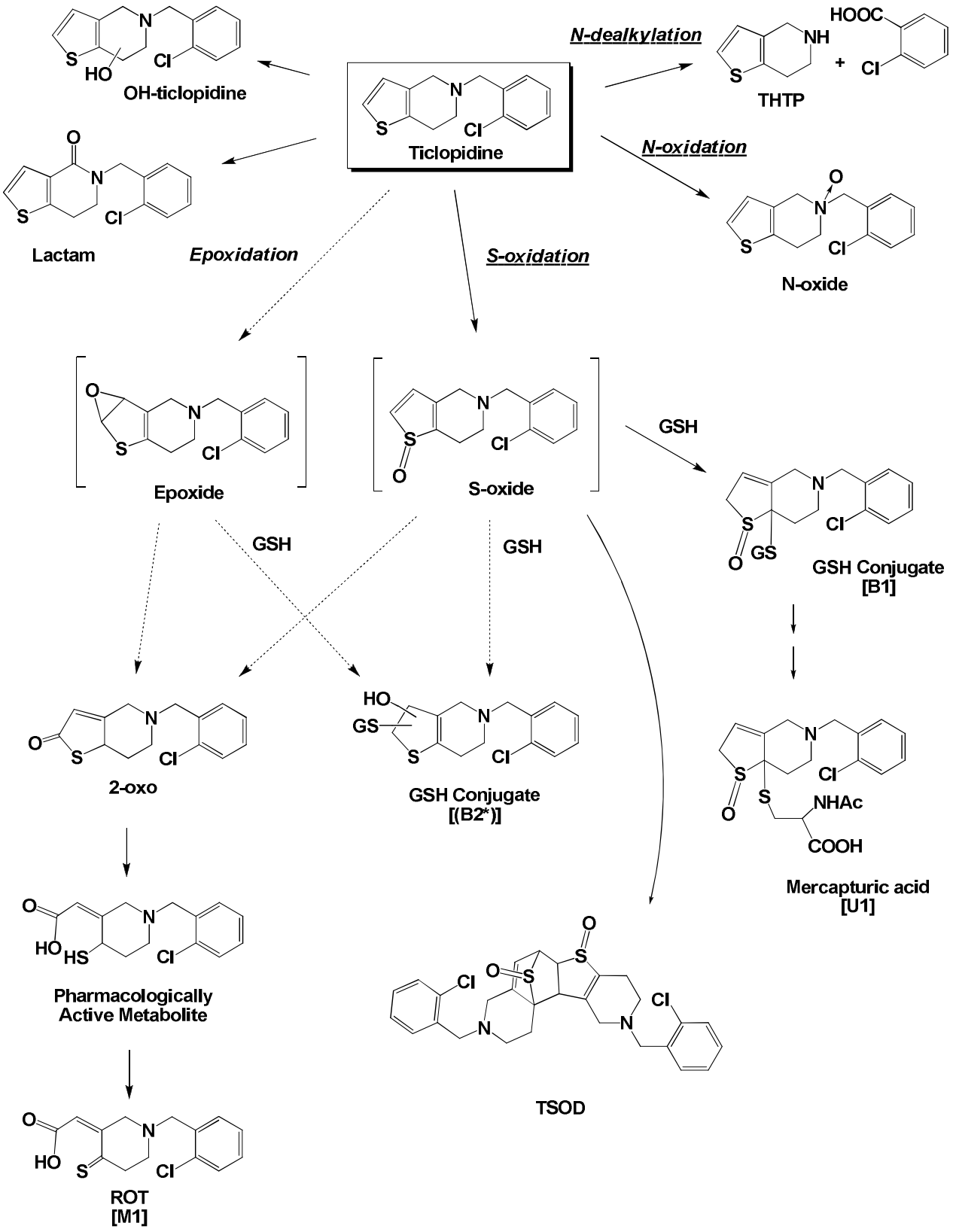

FIG. 13.